Effect of heating of pea fibres on their swelling, rheological properties and in vitro colon fermentation

Food Hydrocolloids 147 (2024) 109306

Contents lists available at ScienceDirect

Food Hydrocolloids

journal homepage: www.elsevier.com/locate/foodhyd

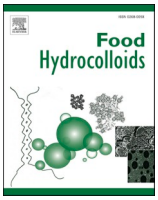

Effect of heating of pea fibres on their swelling, rheological properties and in vitro colon fermentation

Jakob Karlsson [a], Patricia Lopez-Sanchez [b], Tatiana Milena Marques [c], Tuulia Hyötyläinen [d], Victor Castro-Alves [d], Annika Krona [e], Anna Ström [a,*]

[a] Applied Chemistry, Department of Chemistry and Chemical Engineering, Chalmers University of Technology, Gothenburg, Sweden
[b] Food Technology, Department of Analytical Chemistry, Nutrition and Food Science, University of Santiago de Compostela, Campus Terra, Spain
[c] School of Medical Sciences, Faculty of Medicine and Health, Örebro University, Örebro, Sweden
[d] School of Science and Technology, Faculty of Business, Science and Engineering, Örebro University, Sweden
[e] RISE Research Institutes of Sweden, Agriculture and Food, Box 5401, Gothenburg, Sweden

ARTICLE INFO

Keywords:
Pea hull fibre
In vitro colonic fermentation
Rheology

ABSTRACT

Dietary fibre intake is essential for all human beings and has been correlated to beneficial health effects. Pea hull fibres (PF) are generally seen as a side stream during extraction of protein and starch from yellow pea but could be used in various food products to boost fibre content. In this study, the thermal treatment of pea hull fibres was investigated in terms of physicochemical properties and *in vitro* colonic fermentation. The PF that was subjected to heating showed an increase of fibres solubilised in the liquid and particle size. Results also showed that viscosity and storage modulus increased with thermal treatment, possibly due to the swelling of the PF. The pea fibre was readily fermentable based on total gas production and pH. However, the susceptibility to fermentation of PF did not increase with thermal treatment. Total gas production and short chain fatty acid produced were similar independent of thermal treatment. Conclusively, heating of the PF resulted in increased ability to structure water suspension, owing to increased fibre particle size, but is not sufficient to increase short chain fatty acid production during colonic fermentation. To explain this, we propose that the changes in cell wall structure were not major enough to induce higher fermentability.

1. Introduction

A healthy diet includes a dietary fibre intake of 25 g/day (EFSA Panel on Dietetic Products & Allergies, 2010), a level that few citizens and populations meet (Stephen et al., 2017). High amounts of dietary fibres are present in a variety of different plants, such as cereals, vegetables, and pulses (Dhingra, Michael, Rajput, & Patil, 2012; Martens, Nilsen, & Provan, 2017).

Field pea (*Pisum sativum* L.*)* is one of the most studied protein sources due to its high protein content (20–30%) (Boukid, Rosell, & Castellari, 2021; Roy, Boye, & Simpson, 2010), as well as starch (50–60%) and dietary fibres (15–25%) (Pelgrom, Boom, & Schutyser, 2015; Tiwari & Singh, 2012). The dietary fibre fraction is often regarded as side stream from protein and starch extraction (Morales-Medina, Dong, Schalow, & Drusch, 2020).

A majority of the dietary fibres are present in the hull and are often classified as water-insoluble, while the cotyledon fibres consist of both soluble and insoluble fibres (Dalgetty & Baik, 2003; Tosh & Yada, 2010). The main composition of cotyledon fibres is arabinose-rich pectins and hemicelluloses (Reichert, 1981). Cellulose is believed to make up a large portion of the hull fibres, together with smaller fractions of hemicelluloses (xyloglucan and arabinoxylan) and pectins (Ramirez, Temelli, & Saldaña, 2021; Reichert, 1981; Weightman, Renard, & Thibault, 1994).

Pea hull fibres have poor techno-functional properties, such as water-retention capacity (WRC), which relates to their swelling capacity. Swelling capacity of pea hull fibres is lower (1.88 ml/g) than for insoluble cotyledon pea fibres (5.56 ml/g) (Dalgetty & Baik, 2003), but can be increased by reducing the particle size (Auffret, Ralet, Guillon, Barry, & Thibault, 1994) and WRC through microfluidization (Morales-Medina et al., 2020). The WRC for untreated pea hull fibres is low (3.8 g/g) compared to insoluble cotyledon fibre (Dalgetty & Baik, 2003) and fibres from citrus and apple (Robertson et al., 2000).

Pea fibres are, similar to other dietary fibres, non-digestible by

* Corresponding author.
E-mail address: anna.strom@chalmers.se (A. Ström).

https://doi.org/10.1016/j.foodhyd.2023.109306
Received 8 August 2023; Received in revised form 14 September 2023; Accepted 18 September 2023
Available online 19 September 2023

humans but fermented by microbiota in the large intestine (Guillon, Renard, Hospers, Thibault, & Barry, 1995; Titgemeyer, Bourquin, Fahey, & Garleb, 1991). The microbial community uses the dietary fibres as an energy source, and thereby producing short chain fatty acids (SCFAs) (Gill, van Zelm, Muir, & Gibson, 2018; Lu, Flanagan, Mikkelsen, Williams, & Gidley, 2022), where the three main SCFAs produced are acetate, propionate, and butyrate (Koh, De Vadder, Kovatcheva-Datchary, & Bäckhed, 2016). The gut microbiota is important for well-being, and changes in its composition and function have been linked to various illnesses such as allergies, obesity and inflammatory bowel disease (IBD) (Clemente, Ursell, Parfrey, & Knight, 2012). This gives rise to the importance of understanding how food structure and macromolecules affect colon fermentation.

When analysing fermentation of dietary fibres, purified systems has commonly been used, e.g., commercial pectin, which consists mainly of homogalacturonan or resistant starch, in preference of more complex structure (Wang et al., 2019). A more complex system could be a whole cell structure or cell walls consisting mainly of dietary fibres (Stewart & Slavin, 2009). Bhattarai and co-workers examined how treatment of pea cotyledon cell walls can affect pig faecal *in vitro* fermentation. Results showed that broken cell walls treated at lower temperature (60 °C for 1 h) fermented quicker than non-treated cell walls. Therefore, the fermentation of products containing both non-treated and broken cell walls cannot be predicted based on cell wall components and macronutrient content, as the processing needs to be taken into consideration (Bhattarai et al., 2021). Similarly, it has been demonstrated that it is not only components of the cell wall fibre determining the fermentation, but also the size and structure of the particle (Yao, Flanagan, Williams, Mikkelsen, & Gidley, 2023). The accessibility of the particle surface area, and particle structure in terms of compactness or porosity could be the explanation for this. The fermentation of proteins, starch and lipids trapped inside the cell structure could also affect the outcome in terms of SCFA- and gas production. For example, Widaningrum and co-workers observed that macronutrients within the cell walls of legumes and nuts can affect *in vitro* fermentation of cell wall fibres. The authors showed that fermentation of trapped starch granules occur after 12 h when the outer cell wall material had been fermented, leading to a rapid increase in gas production while presence of lipids previously trapped within the cell could inhibit bacterial fermentation (Widaningrum et al., 2022).

The aim of this study was to investigate if thermal treatment of pea hull fibres at 95 °C will affect swelling, solubilization of fibres, rheological properties, and *in vitro* colonic fermentation. The physicochemical and microstructural properties of the systems were determined through chemical characterisation, rheology, and light microscopy. Microscopy was performed before and after *in vitro* colonic fermentation. The fermentation took place *in vitro* under anaerobic conditions to simulate the environment in the large intestine.

2. Materials and methods

2.1. Materials

Yellow pea hull fibre was Vestkorn Fibradan® F20X (Vestkorn Milling A/S, Denmark) with 89.5% total dietary fibres on dry basis. All chemicals used were obtained from Merck (Darmstadt, Germany) if not otherwise stated and were of analytical grade. A total starch assay was purchased from Megazyme Ltd, Bray, Ireland.

2.2. Sample preparation

Thermally treated (T) and non-thermally treated (NT) samples were prepared by dispersing 1–15% (w/v) yellow pea hull fibre flour (PF). Briefly, 51.17 g of sample was added to 300 ml of deionized water to obtain a 15% (w/v) dispersion and homogenized with Silverson L5M-A (7000 rpm for 2 min) (Chesham, UK) and T18 digital ULTRA-TURRAX (16 000 rpm for 1 minte) (IKA Works GmbH & Co. KG, Staufen, Germany) to reduce particle size and increase dispersibility of the samples. The 15% (w/v) dispersion was diluted with deionized water to obtain lower concentrations when needed. The T sample was further subjected to treatment by heating 30 ml of dispersion in a 95 °C water bath for 30 min.

Soluble samples were prepared by centrifuging 30 ml of T and NT samples at 8000 g for 10 min. The supernatant was separated and heated to 95 °C in an oven for 24 h to remove moisture. Residual mass was weighted and kept for further analysis.

2.3. Compositional analysis

2.3.1. Starch

Total starch content was determined according to AOAC Method 996.11 using a total starch assay kit (α-amylase/amyloglucosidase) from Megazyme Ltd, Bray, Ireland.

2.3.2. Monosaccharides

The monosaccharide composition of PF was determined using a modified method described by Sluiter and co-workers (Sluiter et al., 2008). Briefly, 200 ± 0.3 mg of sample was added to a 150 ml beaker, followed by 3 ml of 72% H_2SO_4. The dispersion was placed under vacuum for 15 min. The sample was immersed in a water bath for 1 h at 30 °C. The sample was stirred every 20 min without removing the beaker from the water bath. Thereafter, 84 g of deionized water was added and autoclaved at 125 °C for 1 h. The sample was then vacuum filtered and diluted to a total volume of 100 ml. Further dilutions of 1:10 and 1:50 with deionized water were performed, when necessary, to meet calibration range of the monosaccharides. Fucose was added as internal standard, at a concentration 400 mg fucose/L. Samples were finally filtered through 0.45 μm filters and poured into HPLC vials. Monosaccharide composition analysis was done using high performance anion exchange chromatography (HPAEC) with a pulsed amperometry detector (PAD) (ICS 3000 Dionex, Sunnyvale, USA) equipped with an AEC column (CarboPac PA 1 analytical 4 × 250 nm). Milli-Q (MQ) was used as solvent. Between the injections, 60% v/v 200 mM NaOH and 40% v/v 200 mM NaOH +170 mM NaOAc was run as cleaning. Post column 200 mM of NaOH was added to the flow (0.13 ml/min). Standards used were D (+) glucose, D (+) xylose, D (+) galactose, L (+) arabinose, L (+) rhamnose and D (+) mannose. All samples were measured in duplicates.

2.3.3. Uronic acids

Uronic acid analysis was done according to Liu et al. (Liu, Lopez-Sanchez, Martinez-Sanz, Gilbert, & Gidley, 2019) with some modifications. Shortly, 10.3 ± 0.4 mg sample was weighed into a 10 ml glass tube. The samples were kept on ice and 0.5 ml 96% H_2SO_4 was added twice with 5 min vortex intermittently. Thereafter, the sample were diluted with 0.25 ml of deionized water twice with 5 min vortex intermittently. Deionized water was then added to a total volume of 10 ml.

20 μl of 4 M sulfamic acid-potassium sulfamate (pH 1.6) was added to 1.5 ml plastic Eppendorf tubes together with 160 μl hydrolysed sample. 800 μl 12.5 mM borax in 96% H_2SO_4 was added to the tubes followed by heating at 95 °C for 20 min in an oven. Samples were then cooled and measured on a UV–Vis spectrophotometer (Cary 60 UV–Vis Spectrophotometer, Agilent Technologies, Santa Clara, USA) at 525 nm as a blank. 40 μl of 0.15% (w/v) 3-phenylphenol in 0.5% (w/v) NaOH was added to the samples and measured at 525 nm. Standard curve was constructed using D (+) galacturonic acid (0, 40, 80, 120, 160, 200 μg/ml). All samples were measured in duplicates.

2.4. Characterisation of PF dispersions

2.4.1. Particle size

The particle size distribution (PSD) was measured using Mastersizer;

2000 (Malvern Instruments Ltd, Malvern, UK) equipped with a 2000 Hydro-SM accessory, filled with 100 mL of deionized water. A few droplets (approximately 0.5 mL) of each sample were pipetted into the water. The particle size distribution was determined using a refractive index of 1.47, an absorption of 0.01 and obscuration range 5–10%. Since the particles in the dispersions are rather anisotropic in shape, the model for irregular particles was selected. The PSD was calculated from the intensity profile of the scattered light using the instrument software (Mastersizer 2000; version 6.01). The volume-based $D_{[4,3]}$ and surface area-based $D_{[3,2]}$ average diameters were obtained for every sample, with equations (1) and (2) respectively.

$$D_{[4,3]} = \sum_i n_i d_i^4 \Big/ \sum_i n_i d_i^3 \quad \text{eq. 1}$$

$$D_{[3,2]} = \sum_i n_i d_i^3 \Big/ \sum_i n_i d_i^2 \quad \text{eq. 2}$$

2.4.2. Rheology

The rheological measurements were performed on a DHR-3 (TA Instruments, New Castle, USA) equipped with a 40 mm diameter parallel plate geometry. The gap was set at 1 mm, and the temperature was controlled using a Peltier plate. Evaporation from the samples was avoided using a plate equipped with a solvent trap and custom-built cover from TA Instruments. Flow measurements were done at six concentrations (1, 2, 4, 8, 10 and 15 wt %) in water and carried out at 20 °C. The shear rate ranged from 0.01 s^{-1} to 100 s^{-1}. The samples were stirred covered with aluminium foil at 20 °C, for 24 h prior to measurement.

Oscillatory measurements were carried out at 15 wt %. The sample was added to the rheometer at 20 °C and heated to 95 °C, with 5 °C/min, held at 95 °C for 30 min, and then cooled to 20 °C with 1 °C/min, followed by a frequency sweep ranging from 0.01 rad/s to 100 rad/s at 20 °C and 0.5% strain amplitude.

2.5. Microstructural characterization

2.5.1. Sample preparation

Frozen pellets collected, before and after *in vitro* fermentation, were cut into 8 μm thick sections in a Leica CM3050S cryostat. Sections were applied to Polysine® microscope slides (VWR International, Radnor, USA)

2.5.2. Light microscopy analysis

Sections were mounted in water before examined with an Olympus BX53 light microscope (Olympus Life Science, Tokyo, Japan) with an 10x objective, using differential interference contrast (DIC) imaging to increase the contrast of different structures. Micrographs were captured with a CMos SC50 camera (Olympus Life Science) and processed with the Olympus software cellSense Entry.

2.5.3. Immunolabelling and confocal laser microscopy analysis

For immunolabelling, sections were fixated for 30 min in 4% paraformaldehyde in PBS buffer (pH 7.4) and rinsed with PBS. The sections were then pre-incubated 40 min in PBS buffer with 2.5% BSA before applying the primary antibody LM11 (Plant Probes, Leeds, United Kingdom), directed to arabinoxylan/xylan, diluted 1:50 in PBS containing 0.5% BSA, for 2 h. Negative control were made by replacing the primary antibody solution with PBS containing 0.5% BSA (not shown). After incubation, the sections were rinsed thoroughly with PBS and then incubated for 2 h in the dark with fluorescently labelled secondary antibody Alexa Fluor 647 (Invitrogen, Carlsbad, CA, United States) diluted 1:300 in PBS containing 0.5% BSA. All incubations were performed in moisturized chambers at room temperature. Sections were then rinsed with PBS and mounted with ProLong Diamond (Invitrogen, Carlsbad, CA, Untied States) anti-fading reagent. Micrographs were acquired using a confocal laser microscopy (CLSM; Leica TCS SP5, Heidelberg, Germany) A 488 nm argon laser and a 633 nm HeNe laser with a HCX PL APO lambda blue 20.0x 0.70 IMM UV objective. Emissions were collected at 500–550 (auto-fluorescence shown in green) and 650–700 nm (arabinoxylan/xylan shown in red). Image format 1024x1024 pixels, eight lines average.

2.6. In vitro colonic fermentation

2.6.1. Preparation of medium and substrate

A total volume of 1500 ml medium containing basal solution, phosphate buffer, bicarbonate and vitamins was prepared, see Supplementary Table S1 for full basal media composition and concentrations. The medium had essential nutrients (nitrogen, vitamins, and minerals) for bacterial growth but no added carbon source. The medium was aliquoted by adding 89 ml to 11 different 500 ml Schott bottles and sterilized by autoclaving at 121 °C for 20 min. To remove oxygen the medium was bubbled with nitrogen for 45 min and 1 ml of reducing agent was added.

There were two substrates subjected to *in vitro* fermentation, one thermally treated and one non-thermally treated. For the thermally treated substrate, three ml of pre-prepared solutions of 15 wt % fibre was mixed at 20 °C for 1 h, then added to a metal cylinder and heated at 95 °C for 30 min in a water bath. The substrates were then cooled at room temperature overnight. The non-thermally treated substrates were stirred at 20 °C for 1 h. Substrates were sterilized in a laminar airflow (LAF) bench using UV-light for 30 min. In sterile conditions two g of each substrate were weighed into separate 50 ml falcon tubes and closed. Each substrate was prepared in triplicate.

2.6.2. Faecal inoculum preparation

The inoculum was prepared in a LAF bench under sterile conditions. Faeces were donated by three human volunteers with unrestricted diets and no reported gastro-intestinal diseases. The experiment was run in triplicate, with three separate donors for each experiment run. The faeces were diluted to 20 wt % in 50 mM phosphate buffer solution, homogenized and filtered through a sieve bag. Preparation of the inoculum occurred within 2 h of the faecal collection. Experiments were conducted following ethical guidelines approved by the Swedish Ethical Review Authority (2022-01696-01).

2.6.3. In vitro fermentation

To each substrate 10 ml faecal inoculum was added and mixed on a vortex, and the substrate and faecal inoculum mixture was transferred using a syringe into bottles containing the anaerobic medium. The total volume was 100 ml. The bottles were kept at 37 °C for 24 h with sampling at 0, 8 and 24 h. The samples were centrifuged after each sampling at 4 °C and 18 000 rpm to stop the fermentation process and separate the pellet and supernatant. The pH was measured in the supernatant, and the samples were stored at −80 °C until further use. Total gas produced was measured over time in each bottle using the Gas Endeavor system (Bioprocess Control). Moreover, a blank containing only the medium and faecal inoculum was included in the experiment.

2.6.4. Short chain fatty acid (SCFA) analysis

To confirm the *in vitro* fermentation functionality, the levels of acetate, propionate, and butyrate were monitored at various time points (0, 8 and 24 h). The analysis of SCFAs was conducted using UHPLC-qToF-MS after applying the 3-nitrophenylhydrazin (3-NPH) derivatization method, as previously described by (Dei Cas et al., 2020). Briefly, an aliquot (50 μL) of the fermentation extract was mixed with cold methanol (90 μL) containing the internal standards (IS, 10 μg/mL each) aceticacid-d4, butyric acid-d8 and propionic acid-d2. The extract was ultrasonicated (5 min), and then centrifuged (10 000 g, 5 min, 4 °C) and transferred (100 μL) to an LC vial. For derivatization, the sample was mixed with 50 mM 3-NPH (50 μL), 50 mM N-ethylcarbodiimide (EDC,

50 μL), and 7% pyridine (50 μL). Following an incubation period of 1 h, the derivatization reaction was stopped by adding 0.2% formic acid, and the sample was immediately subjected to UHPLC-qToF-MS analysis.

The UHPLC system was equipped with an Acquity BEH C18 column (2.1 × 100 mm, 1.7 μm; Waters) using mobile phase A as 0.1% formic acid in water and mobile phase B as acetonitrile. The elution gradient (0.4 ml/min) started at 10% MPB (0–2 min), followed by a linear increase to 100% MPB (2–4 min), maintaining 100% MPB (4–6 min), and then re-equilibrating with 10% MPB for 4 min. The column temperature was set at 50 °C, while the autosampler temperature was maintained at 10 °C. The mass spectra were acquired (2 spectra/s) in negative ion mode with an m/z range of 70–1500. The parameters for the ESI source were set as follows: collision energy 0 V, capillary voltage 3.6 kV, nozzle voltage 1500 V, and N2 pressure at nebulizer, flow rate, and temperature as sheath gas set at 21 psi, 10 L/min, and 379 °C, respectively. The injection volume was 5 μL. Data acquisition and processing were performed using MassHunter Workstation Software (Agilent).

2.7. Statistical analysis

All rheological measurements were done in duplicate, with the figures showing the mean value. Error based on the mean was less than 10%, indicating good reproducibility. Particle size and SCFA production were evaluated with a one-way analysis of variance (ANOVA) with a significance of $p < 0.05$.

3. Results and discussion

3.1. Compositional analysis

The total starch content of the PF fraction was 1.3 g/100 g. The monosaccharide analysis showed that the majority of the polysaccharides in the PF consist of glucose (61.5%) (Table 1). The low starch content indicates that the larger portion of glucose obtained in the monosaccharide analysis originates from cellulose, which agrees with previous literature (Ralet, Della Valle, & Thibault, 1993; Weightman et al., 1994).

The second and third most prominent monosaccharides in the PF fraction are xylose (15.5%) followed by arabinose (5.6%). This implies the presence of polysaccharides with a high amount of xylose and some arabinose, e.g. xyloglucan and arabinoxylan, in agreement with proposed pea hull fibre composition by Ralet and co-workers (Ralet, Saulnier, & Thibault, 1993) and later also Ramirez and co-workers (Ramirez et al., 2021). The presence of xyloglucan, which commonly form structures with cellulose in cell walls, can also be a source of the determined glucose (Pauly, Albersheim, Darvill, & York, 1999). The small soluble part of the pea hull fibres has been shown to contain a majority of pectic substances, but also a lowly branched xylan and a free arabinan (Ralet, Saulnier, & Thibault, 1993). Uronic acid, as found here at a level of 13.6%, is indicative of pectic polysaccharides. Uronic acid in pea hull fibre is mainly galacturonic acid (97%) with only a small amount of glucuronic acid (3%) (Weightman et al., 1994). The PF also contained small amount of galactose (2%) and rhamnose (1.8%), which may originate from rhamnogalacturonan-I (Ramirez et al., 2021; Weightman, Renard, Gallant, & Thibault, 1995).

Table 1
Monosaccharide composition of the whole PF fraction in wt % of total monosaccharides, as well as determination of solubilised PF fraction before (NT) and after (T) thermal treatment at 95 °C for 30 min.

Monosaccharide	PF	Soluble NT	Soluble T
Arabinose	5.6	14.1	14.3
Galactose	2.0	12.9	10.5
Glucose	61.5	5.5	15.2
Mannose	tr	tr	tr
Rhamnose	1.8	4.1	4.9
Xylose	15.5	15.4	13.3
Uronic acids	13.6	47.9	41.7

tr: traces (<1 mg/L).

The amount of soluble fibre was 2.0 g/100 g for the NT sample and 3.1 g/100 g in the T sample. An increase from 2.0% to 3.1% indicates a release of soluble fibres or starch after thermal treatment. Most monosaccharide fractions remained constant between NT and T samples (Table 1). The glucose fraction increased from 5.5% to 15.2% after thermal treatment, implying solubilization of part of the starch fraction. Uronic acid makes up the major portion of the soluble fibres (47.9% and 41.7%), probably originating from pectic polysaccharides.

3.2. Particle size

For sample preparation, mechanical treatment was used to increase dispersibility. Before preparation, clear sedimentation of the pea hull fibre occurred. After mechanical treatment, pea hull fibres in dispersion have an irregular shape (Fig. 1). Differences in particle size ($D_{[3,2]}$ and $D_{[4,3]}$) between the NT and T pea fibres could be observed using laser diffraction (Fig. 1). Non-heated PF had a $D_{[3,2]}$ value of 98 μm which was statistically smaller compared to heated PF with $D_{[3,2]}$ of 116 μm. Similarly, a statistically significant difference in $D_{[4,3]}$ values were found between non-heated and heated, with values of 310 and 326 μm respectively.

3.3. Rheology

The viscosity of six different PF concentrations was measured, ranging from 1 to 15% (w/v) (Fig. 2). The viscosity increased with PF concentration for both non-heated and heated samples. A general increase in the viscosity as a function of concentration is due to larger volume fraction (φ) of the PF. The PF behaves as a dilute system at low concentrations or low φ, with the particles having little to no effect on the viscosity. This is observed at specifically 1–2% (w/v), and independent of PF being thermally treated or not. At higher PF concentrations, the system becomes shear-thinning and exhibits the behaviour of concentrated dispersions, and eventually reach a volume fraction above the critical packing fraction (φ_c), where solid-like properties are displayed (Fig. 3) (Dames, Morrison, & Willenbacher, 2001). For both NT and T dispersions, the φ_c is around 5% (w/v). Main parameters influencing the rheological properties are hydrodynamic interactions and particle-particle interactions (Dobias, Qiu, & von Rybinski, 1999). The latter plays a larger part when the volume fraction increases as more interactions between the particle occurs. In the case of PF, little to no electrostatic interactions are expected due to the negative charge of the particles (−20 mV), but interactions will still occur at higher φ due to steric hindrance. Based on the particle size results, the size distribution is wide resulting in a higher packing density compared to a monodisperse system. The packing density is higher because smaller particles can fill voids between larger ones, increasing interactions between particles (Dobias et al., 1999). In addition, the morphology of the PF is irregular further reducing the needed volume fraction for particle-particle interactions, as the effective volume fraction is much larger during rotation compared to symmetrical morphology. The observed higher viscosity for the heated PF is in line with the particle size measurements indicating swelling of the PF upon heating.

Rheological properties of the PF dispersion at 15% (v/w) during heating was measured (Fig. 3). Before starting the temperature ramp, G' is larger than G'', indicating a paste-like system. During heating to 95 °C, and the sequential cooling down, G' and G'' increases steadily until a plateau is reached at 20 °C. In the heating process, G' increases after cooling, implying larger contribution from elastic components upon thermal treatment. The higher elasticity in the system probably stems from the swelling of PF particles, and thereby increase in volume fraction. A larger particle size would increase the volume fraction of the PF dispersion and consequently make the system behave more solid-like.

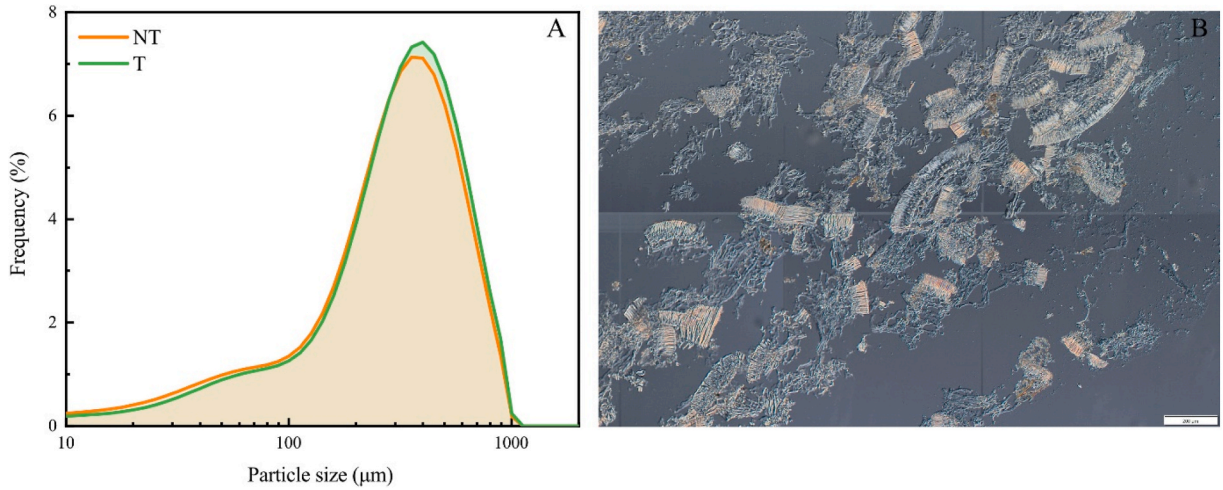

Fig. 1. A. Particle size distribution of non-thermally (orange) and thermally (green) treated pea fibre dispersions. B. Light microscopy micrograph, using DIC imaging, showing the particles in non-thermally treated sample. Scale bar represent 200 μm.

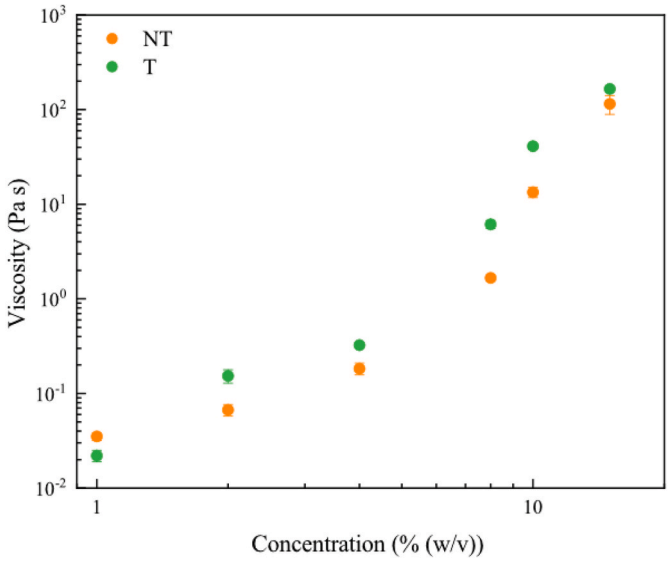

Fig. 2. Viscosity as a function of concentration of PF dispersions at T = 25 °C and shear rate of 10 s^{-1}. Average value and error bars are based on three measurements. Error bars are smaller than the symbol when not visible.

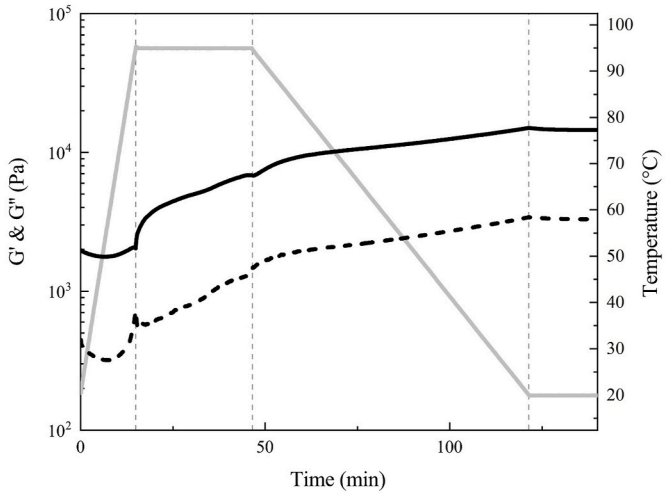

Fig. 3. Elastic modulus (G′) depicted as black line, and viscous modulus (G″) depicted as dashed black line of pea fibre (PF) dispersion at 15% (w/v) during temperature ramp (grey line).

The solubilised polysaccharides released during heating could also be a possible explanation for the increased viscosity. However, the concentration of soluble fibres present in the dispersion is still low, and thereby negligible. Viscosity measurements on the solubilised fibre fraction was performed, and it displayed Newtonian behaviour with low viscosity. The rheological properties of the pea fibres studied here, is dominated of what would be expected from a particulate gel.

3.4. *In vitro colonic fermentation*

pH was measured at 0, 8 and 24 h to assess if fermentation occurred. When SCFA are produced, the pH will decrease and thereby give an indication of the fermentation. The pH decreased significantly for the NT and T samples over 24 h. The pH of NT sample was pH 7.39 ± 0.14 before fermentation started, 6.56 ± 0.11 at 8 h, and it was 6.05 ± 0.49 after 24 h. Similarly, for T samples, the pH decreased from 7.28 ± 0.07 to 6.39 ± 0.02 after 8 h. The pH was 5.84 ± 0.25 after 24 h for the T sample. While the average pH of the thermally treated samples was lower, there was no significant difference between the NT and T samples.

Fermentation of dietary fibres results in production of gases (mainly CO_2 and H_2) which gives an outlook the rate and extent of the fermentation process. The NT and T samples produced comparable cumulative gas totals with 45.7 ml/g and 44.2 ml/g respectively (Fig. 4). Previous papers have reported lower or similar values in gas production for pea hull fibres (Cherbut, Salvador, Barry, Doulay, & Delort-Laval, 1991; Guillon et al., 1995; Lebet, Arrigoni, & Amado, 1998). Other studied polysaccharides with high fermentability, such as pectin and xyloglucans, produce around 150–200 ml/g gas over 24 h, while pure cellulose has a lower gas production at 25 ml/g (Lu et al., 2022). High cellulose content of PF could be an explanation for the low susceptibility to fermentation.

3.5. *Short chain fatty acid production*

The end-products from dietary fibre fermentation are SCFA. Total SCFA produced and proportions of acetate, propionate and butyrate are shown in Table 2. Highest total amount of SCFA at 24 h was observed in the T sample (1.3 mmol/g), however only slightly larger than in the NT sample (1.1 mmol/g). Both samples showed an increase in total amount

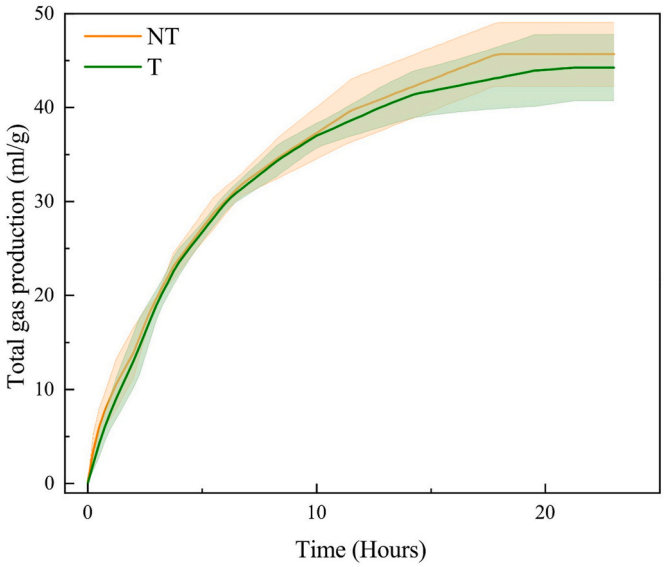

Fig. 4. Total gas production per gram substrate of non-thermally (NT) and thermally (T) treated samples during *in vitro* colonic fermentation.

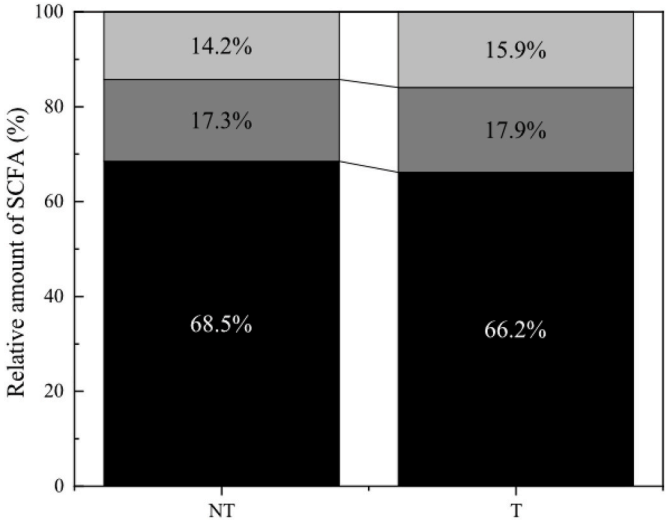

Fig. 5. Relative fractions of acetate (black), propionate (dark grey) and butyrate (light grey) produced at 24 h for non-thermally (NT) and thermally (T) treated samples of *in vitro* colonic fermentation.

Table 2
Average acetate, propionate, butyrate and total SCFA produced for NT and T samples at 8 and 24 h for the three donors. Values are presented in mmol per gram sample (mmol/g).

Sample	NT		T	
Time (h)	8	24	8	24
Acetate	0.47 ± 0.13	0.76 ± 0.21	0.55 ± 0.04	0.87 ± 0.09
Propionate	0.11 ± 0.06	0.19 ± 0.12	0.14 ± 0.02	0.23 ± 0.03
Butyrate	0.09 ± 0.06	0.16 ± 0.10	0.10 ± 0.01	0.21 ± 0.02
Total SCFA	0.67 ± 0.25	1.11 ± 0.43	0.79 ± 0.08	1.31 ± 0.13

SCFA from eight to 24 h. Donor 2 produced less total SCFA compared to donor 1 and 3 (Supplementary Table S2). The deviation in total SCFA observed between the donors could be related to differences in microbiota composition (Eckburg et al., 2005). All samples produced significantly more SCFA compared to control (faecal inoculum without substrate, Supplementary Table S3).

Relative amounts of SCFA produced for NT and T samples at 24 h are almost identical (Fig. 5). Higher acetate fraction was observed in the NT sample, compared to T sample which had larger propionate and butyrate production. Production of acetate has been correlated to fermentation of uronic acid (Lu et al., 2022; McBurney & Thompson, 1989; Salvador et al., 1993). Relatively large acetate proportions (68.5% and 66.2% respectively) could be due to the large fraction of uronic acid in PF and its susceptibility to fermentation compared to other polysaccharides present. The slightly higher values of propionate and butyrate in the T sample could be due to increased solubility of glucose containing polysaccharides. Fermentation of polymeric and monomeric glucose has shown to produce high amounts of propionate (Barry, Chourot, Bonnet, Kozlowski, & David, 1989). Furthermore, xylose when fermented has been correlated to production of butyrate.

3.6. Microstructural analysis during in vitro colonic fermentation

Arabinoxylan was immunolabelled to better distinguish details in the hull (Fig. 6.). Most arabinoxylan and xylan-containing polysaccharides are located in the outer part of the hull. Small or no difference in fibre microstructure was observed before and after fermentation. Supplementary Figs. S1 and S2 show representative images for donors 1 and 3, as well.

The present study suggests that pea hull fibres consist of a small soluble fraction (2 g/100 g), which was increased by thermal treatment (3.1 g/100 g). Earlier reports have shown similar results with small soluble fractions in unheated pea hull fibre (Ralet, Saulnier, & Thibault, 1993; Ramirez et al., 2021). While the thermal treatment increases the fraction of solubilised fibres, the viscosity of the PF suspension was still dominated by insoluble particles. A significant increase in G' was observed after heating step (five-fold increase), a result of particle swelling, thus resulting in a higher volume fraction (φ).

Low fermentability of pea hull fibres has been reported previously (Guillon et al., 1995; Lebet et al., 1998; Salvador et al., 1993). Fermentation of dietary fibres are dependent on what types of polysaccharides are present, their linkages to each other and the structure of the cell wall. High cellulose content and crystallinity in pea hull fibres have been given as a main reason for the low susceptibility to fermentation. The fermentation of pea hull fibres did not change significantly with thermal treatment, even if differences were observed in particle size and rheological measurements. Swelling of the particles could have made parts of the fibre more approachable for the microbiota, but due to the large cellulose content (which would be mostly unaffected by heating), the fibre remains insusceptible to fermentation. (Lu, Mikkelsen, Flanagan, Williams, & Gidley, 2021). The interaction between individual polysaccharides within the cell wall structure would therefore affect the fermentation outcome. The presence of dietary fibres in the large intestine is important as they constitute fermentable substrates, as well as binds water and contribute to stool consistency (Cherbut et al., 1991).

4. Conclusion

The pea hull fibre contained a majority of cellulose, but also a large portion of uronic acids. Only a small part of the present fibres was soluble but increased from 2.0% to 3.1% with thermal treatment. Significant increase in particle size could be observed after thermal treatment, probably due to swelling of broken cell walls. Similarly, viscosity and storage modulus displayed higher values after heating, due to the increase in particle size of broken cell walls, rather than increase in soluble fibres.

The pea hull fibres are fermented by the microbiota, producing acetate (~68%), propionate (17–18%) and butyrate (14–16%). Heat treatment did not affect the fermentation of pea hull fibres significantly, but small differences in SCFA proportions could be observed. A slight

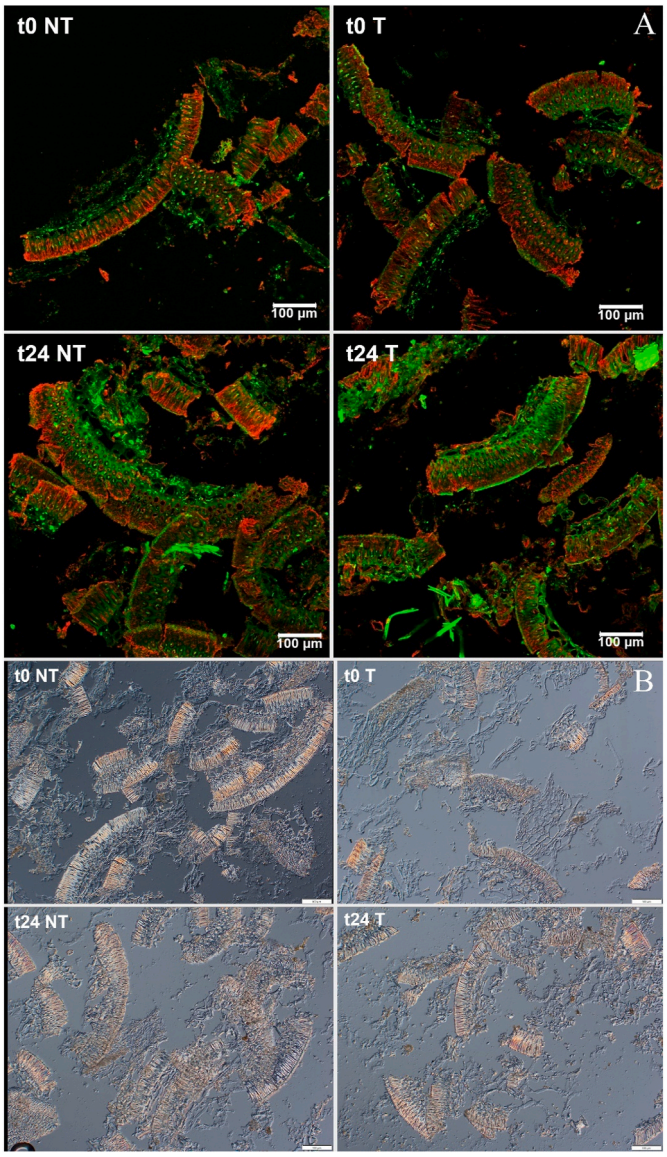

Fig. 6. Micrographs of non-thermally and thermally treated pea fibres, before and after fermentation from donor 2. Scale bars 100 µm. A: CLSM micrographs showing arabinoxylan/xylan in red and auto-fluorescence in green. A: Top row is non-thermally (NT) and thermally (T) treated samples at 0 h. Bottom row is NT and T samples after 24 h of *in vitro* colonic fermentation. B: Light microscope micrographs using DIC imaging showing total structures in samples. Top row is NT and T samples at 0 h. Bottom row is NT and T samples after 24 h.

increase in propionate and butyrate fractions were observed for the thermally treated sample.

CRediT author statement

Jakob Karlsson: Validation, Investigation, Visualization, Writing – Original draft. Patricia Lopez-Sanchez: Conceptualization, Investigation, Supervision, Writing – Review & Editing. Tatiana Milena Marques: Conceptualization, Supervision, Writing – Review & Editing. Tuulia Hyötyläinen: Validation, Writing – Review & Editing. Victor Castro-Alves: Validation, Investigation. Annika Krona: Supervision, Investigation. Anna Ström: Conceptualization, Supervision, Writing – Review & Editing, Funding acquisition.

Declaration of competing interest

The authors declare that they have no known competing financial interests or personal relationships that could have appeared to influence the work reported in this paper.

Data availability

Data will be made available on request.

Acknowledgements

The study was performed within the PANSweden consortium, which acknowledge financial support from the Swedish research council, FORMAS grant number 2020-02843. We acknowledge Orkla for providing fiber samples.

Appendix A. Supplementary data

Supplementary data to this article can be found online at https://doi.org/10.1016/j.foodhyd.2023.109306.

References

Auffret, A., Ralet, M. C., Guillon, F., Barry, J. L., & Thibault, J. F. (1994). Effect of grinding and experimental conditions on the measurement of hydration properties of dietary fibres. *LWT - Food Science and Technology, 27*(2), 166–172. https://doi.org/10.1006/fstl.1994.1033

Barry, J. L., Chourot, J. M., Bonnet, C., Kozlowski, F., & David, A. (1989). In vitro fermentation of neutral monosaccharides by ruminal and human fecal microflora. *Acta Veterinaria Scandinavica Supplementum, 86*, 93–95.

Bhattarai, R. R., Dhital, S., Williams, B. A., Yang, H. J., Mikkelsen, D., Flanagan, B. M., et al. (2021). In vitro fermentation of legume cells and components: Effects of cell encapsulation and starch/protein interactions. *Food Hydrocolloids, 113*, Article 106538. https://doi.org/10.1016/j.foodhyd.2020.106538

Boukid, F., Rosell, C. M., & Castellari, M. (2021). Pea protein ingredients: A mainstream ingredient to (re)formulate innovative foods and beverages. *Trends in Food Science & Technology, 110*, 729–742. https://doi.org/10.1016/j.tifs.2021.02.040

Cherbut, C., Salvador, V., Barry, J. L., Doulay, F., & Delort-Laval, J. (1991). Dietary fibre effects on intestinal transit in man: Involvement of their physicochemical and fermentative properties. *Food Hydrocolloids, 5*(1), 15–22. https://doi.org/10.1016/S0268-005X(09)80281-6

Clemente, J. C., Ursell, L. K., Parfrey, L. W., & Knight, R. (2012). The impact of the gut microbiota on human health: An integrative view. *Cell, 148*(6), 1258–1270. https://doi.org/10.1016/j.cell.2012.01.035

Dalgetty, D. D., & Baik, B.-K. (2003). Isolation and characterization of cotyledon fibers from peas, lentils, and chickpeas. *Cereal Chemistry, 80*(3), 310–315. https://doi.org/10.1094/CCHEM.2003.80.3.310

Dames, B., Morrison, B. R., & Willenbacher, N. (2001). An empirical model predicting the viscosity of highly concentrated, bimodal dispersions with colloidal interactions. *Rheologica Acta, 40*(5), 434–440. https://doi.org/10.1007/s003970100171

Dei Cas, M., Paroni, R., Saccardo, A., Casagni, E., Arnoldi, S., Gambaro, V., … Roda, G. (2020). A straightforward LC-MS/MS analysis to study serum profile of short and medium chain fatty acids. *Journal of Chromatography B, 1154*, Article 121982. https://doi.org/10.1016/j.jchromb.2020.121982

Dhingra, D., Michael, M., Rajput, H., & Patil, R. T. (2012). Dietary fibre in foods: A review. *Journal of Food Science and Technology, 49*(3), 255–266. https://doi.org/10.1007/s13197-011-0365-5

Dobias, B., Qiu, X., & von Rybinski, W. (1999). *Solid - liquid dispersions* (1 ed. Vol. 81). Marcel Dekker, Inc.

Eckburg, P. B., Bik, E. M., Bernstein, C. N., Purdom, E., Dethlefsen, L., Sargent, M., et al. (2005). Diversity of the human intestinal microbial flora. *Science, 308*(5728), 1635–1638. https://doi.org/10.1126/science.1110591

EFSA Panel on Dietetic Products, N. & Allergies. (2010). Scientific opinion on dietary reference values for carbohydrates and dietary fibre. *EFSA Journal, 8*(3), 1462. https://doi.org/10.2903/j.efsa.2010.1462

Gill, P. A., van Zelm, M. C., Muir, J. G., & Gibson, P. R. (2018). Review article: Short chain fatty acids as potential therapeutic agents in human gastrointestinal and inflammatory disorders. *Alimentary Pharmacology & Therapeutics, 48*(1), 15–34. https://doi.org/10.1111/apt.14689

Guillon, F., Renard, C. M. G. C., Hospers, J., Thibault, J.-F., & Barry, J.-L. (1995). Characterisation of residual fibres from fermentation of pea and apple fibres by human faecal bacteria. *Journal of the Science of Food and Agriculture, 68*(4), 521–529. https://doi.org/10.1002/jsfa.2740680417

Koh, A., De Vadder, F., Kovatcheva-Datchary, P., & Bäckhed, F. (2016). From dietary fiber to host physiology: Short-chain fatty acids as key bacterial metabolites. *Cell, 165*(6), 1332–1345. https://doi.org/10.1016/j.cell.2016.05.041

Lebet, V., Arrigoni, E., & Amado, R. (1998). Measurement of fermentation products and substrate disappearance during incubation of dietary fibre sources with human

faecal flora. *Food Science and Technology-Lebensmittel-Wissenschaft & Technologie, 31*(5), 473–479.

Liu, D., Lopez-Sanchez, P., Martinez-Sanz, M., Gilbert, E. P., & Gidley, M. J. (2019). Adsorption isotherm studies on the interaction between polyphenols and apple cell walls: Effects of variety, heating and drying. *Food Chemistry, 282*, 58–66. https://doi.org/10.1016/j.foodchem.2018.12.098

Lu, S., Flanagan, B. M., Mikkelsen, D., Williams, B. A., & Gidley, M. J. (2022). In vitro fermentation of onion cell walls and model polysaccharides using human faecal inoculum: Effects of molecular interactions and cell wall architecture. *Food Hydrocolloids, 124*, Article 107257. https://doi.org/10.1016/j.foodhyd.2021.107257

Lu, S., Mikkelsen, D., Flanagan, B. M., Williams, B. A., & Gidley, M. J. (2021). Interaction of cellulose and xyloglucan influences in vitro fermentation outcomes. *Carbohydrate Polymers, 258*, Article 117698. https://doi.org/10.1016/j.carbpol.2021.117698

Martens, L. G., Nilsen, M., & Provan, F. (2017). Pea hull fibre: Novel and sustainable fibre with important health and functional properties. *EC Nutrition, 10*(4), 139–148.

McBurney, M. I., & Thompson, L. U. (1989). In vitro fermentabilities of purified fiber supplements. *Journal of Food Science, 54*(2), 347–350. https://doi.org/10.1111/j.1365-2621.1989.tb03077.x

Morales-Medina, R., Dong, D., Schalow, S., & Drusch, S. (2020). Impact of microfluidization on the microstructure and functional properties of pea hull fibre. *Food Hydrocolloids, 103*, Article 105660. https://doi.org/10.1016/j.foodhyd.2020.105660

Pauly, M., Albersheim, P., Darvill, A., & York, W. S. (1999). Molecular domains of the cellulose/xyloglucan network in the cell walls of higher plants. *The Plant Journal, 20*(6), 629–639. https://doi.org/10.1046/j.1365-313x.1999.00630.x

Pelgrom, P. J. M., Boom, R. M., & Schutyser, M. A. I. (2015). Functional analysis of mildly refined fractions from yellow pea. *Food Hydrocolloids, 44*, 12–22. https://doi.org/10.1016/j.foodhyd.2014.09.001

Ralet, M. C., Della Valle, G., & Thibault, J. F. (1993). Raw and extruded fibre from pea hulls. Part I: Composition and physico-chemical properties. *Carbohydrate Polymers, 20*(1), 17–23. https://doi.org/10.1016/0144-8617(93)90028-3

Ralet, M. C., Saulnier, L., & Thibault, J. F. (1993). Raw and extruded fibre from pea hulls. Part II: Structural study of the water-soluble polysaccharides. *Carbohydrate Polymers, 20*(1), 25–34. https://doi.org/10.1016/0144-8617(93)90029-4

Ramirez, C. S. V., Temelli, F., & Saldaña, M. D. A. (2021). Production of pea hull soluble fiber-derived oligosaccharides using subcritical water with carboxylic acids. *The Journal of Supercritical Fluids, 178*, Article 105349. https://doi.org/10.1016/j.supflu.2021.105349

Reichert. (1981). Quantitative isolation and estimation of cell wall material from dehulled pea (pisum sativum) flours and concentrates. *Cereal Chemistry, 58*(4), 266–270.

Robertson, J. A., de Monredon, F. D., Dysseler, P., Guillon, F., Amado, R., & Thibault, J.-F. (2000). Hydration properties of dietary fibre and resistant starch: A European collaborative study. *LWT - Food Science and Technology, 33*(2), 72–79. https://doi.org/10.1006/fstl.1999.0595

Roy, F., Boye, J. I., & Simpson, B. K. (2010). Bioactive proteins and peptides in pulse crops: Pea, chickpea and lentil. *Food Research International, 43*(2), 432–442. https://doi.org/10.1016/j.foodres.2009.09.002

Salvador, V., Cherbut, C., Barry, J.-L., Bertrand, D., Bonnet, C., & Delort-Laval, J. (1993). Sugar composition of dietary fibre and short-chain fatty acid production during in vitro fermentation by human bacteria. *British Journal of Nutrition, 70*(1), 189–197. https://doi.org/10.1079/BJN19930116

Sluiter, A., Hames, B., Ruiz, R., Scarlata, C., Sluiter, J., Templeton, D., et al. (2008). Determination of structural carbohydrates and lignin in biomass. In *Laboratory analytical procedure (LAP)*. National Renewable Energy Laboratory.

Stephen, A. M., Champ, M. M. J., Cloran, S. J., Fleith, M., van Lieshout, L., Mejborn, H., et al. (2017). Dietary fibre in europe: Current state of knowledge on definitions, sources, recommendations, intakes and relationships to health. *Nutrition Research Reviews, 30*(2), 149–190. https://doi.org/10.1017/S095442241700004X

Stewart, M. L., & Slavin, J. L. (2009). Particle size and fraction of wheat bran influence short-chain fatty acid production in vitro. *British Journal of Nutrition, 102*(10), 1404–1407. https://doi.org/10.1017/S0007114509990663

Titgemeyer, E. C., Bourquin, L. D., Fahey, G. C., Jr., & Garleb, K. A. (1991). Fermentability of various fiber sources by human fecal bacteria in vitro. *The American Journal of Clinical Nutrition, 53*(6), 1418–1424. https://doi.org/10.1093/ajcn/53.6.1418

Tiwari, B. K., & Singh, N. (2012). *Pulse chemistry and technology*. Royal Society of Chemistry.

Tosh, S. M., & Yada, S. (2010). Dietary fibres in pulse seeds and fractions: Characterization, functional attributes, and applications. *Food Research International, 43*(2), 450–460. https://doi.org/10.1016/j.foodres.2009.09.005

Wang, M., Wichienchot, S., He, X., Fu, X., Huang, Q., & Zhang, B. (2019). In vitro colonic fermentation of dietary fibers: Fermentation rate, short-chain fatty acid production and changes in microbiota. *Trends in Food Science & Technology, 88*, 1–9. https://doi.org/10.1016/j.tifs.2019.03.005

Weightman, R. M., Renard, C. M. G. C., Gallant, D. J., & Thibault, J. F. (1995). Structure and properties of the polysaccharides from pea hulls—II. Modification of the composition and physico-chemical properties of pea hulls by chemical extraction of the constituent polysaccharides. *Carbohydrate Polymers, 26*(2), 121–128. https://doi.org/10.1016/0144-8617(94)00102-Y

Weightman, R. M., Renard, C. M. G. C., & Thibault, J. F. (1994). Structure and properties of the polysaccharides from pea hulls. Part 1: Chemical extraction and fractionation of the polysaccharides. *Carbohydrate Polymers, 24*(2), 139–148. https://doi.org/10.1016/0144-8617(94)90024-8

Widaningrum, Flanagan, B. M., Williams, B. A., Sonni, F., Chen, P., Mikkelsen, D., et al. (2022). In vitro fermentation profiles of undigested fractions from legume and nut particles are affected by particle cohesion and entrapped macronutrients. *Food & Function, 13*(9), 5075–5088. https://doi.org/10.1039/D2FO00250G

Yao, H., Flanagan, B. M., Williams, B. A., Mikkelsen, D., & Gidley, M. J. (2023). Particle size of dietary fibre has diverse effects on in vitro gut fermentation rate and end-products depending on food source. *Food Hydrocolloids, 134*, Article 108096. https://doi.org/10.1016/j.foodhyd.2022.108096